metals

Article

The Effect of Grain Size on the Diffusion Bonding Properties of SP700 Alloy

Qianwen Zhang [1,2], Jianjun Wu [1,*], Shaosong Jiang [3,*] and Gang He [2]

1 School of Mechanical Engineering, Northwestern Polytechnical University, Xi'an 710072, China; zhangqianwen.love@163.com
2 AVIC Xi'an Aircraft Industry Group Company Ltd., Xi'an 710089, China; ganghe0118@163.com
3 School of Materials Engineering, Harbin Institute of Technology, Harbin 150006, China
* Correspondence: wujj@nwpu.edu.cn (J.W.); jiangshaosong@hit.edu.cn (S.J.); Tel.: +86-029-88493101 (J.W.)

Abstract: Superplastic forming and diffusion bonding (SPF/DB) has been recognized as a viable manufacturing technology. However, the basic understanding of grain size and its effects on the quality of diffusion bonds is still limited. In this study, a certain type of SP700 alloy with different grain sizes is bonded at superplastic temperature. The experimental results indicate that the same materials, if coarse-grained, may not readily bond under identical conditions of pressure, temperature, and time. This type of bonding is possible because of the presence of many grain boundaries in fine-grained materials that act as short-circuit paths for diffusion. In addition, grain-boundary migration is also faster in fine-grained than in coarse-grained materials. Fractographic studies show that the dimples on the coarse-grained specimen have large dimensions compared with that in the fine-grained material, indicating that heterogeneous deformation develops in the coarse-grained specimen during tension.

Keywords: diffusion bonding; titanium alloy; grain size; fracture

check for updates

Citation: Zhang, Q.; Wu, J.; Jiang, S.; He, G. The Effect of Grain Size on the Diffusion Bonding Properties of SP700 Alloy. *Metals* **2022**, *12*, 237. https://doi.org/10.3390/met12020237

Academic Editor: C. Issac Garcia

Received: 27 December 2021
Accepted: 21 January 2022
Published: 26 January 2022

1. Introduction

Titanium and its alloys have been widely used in the medical, automotive, and aerospace industries due to their excellent mechanical properties [1–4]. Concurrent superplastic forming and diffusion bonding have been recognized as a viable technology that enables both cost and weight saving compared with conventional methods. Superplasticity refers to the ability of certain alloys to undergo extensive tensile strain at a specific temperature and strain rate [5–7]. Diffusion bonding involves complex boundary migration and plastic deformation [8–11]. While most works currently focused on the superplasticity of steels and ferrous alloys [12–15], very limited research has investigated the diffusion bonding process [16–18]. The microstructure evolutions during the DB would certainly determine the mechanical behaviors of the formed parts [19]; thus, the purpose of this study was to explore the effect of initial materials on the bonding joints microstructures.

At superplastic temperature, the atomic diffusion and particularly the boundary migration are usually rapid. Previous studies investigated the effect of the forming parameters on the mechanical properties of the bonds. For example, Lin et al. [20] performed the diffusion bonding experiment for Ti-6Al-4V alloy; the optimal parameter was chosen between 900 and 950 °C with bonding pressure of 1–5 MPa. Han et al. [21] made the four-layer structure of titanium by gas pressure forming at 930 °C. However, the basic understanding of the surface condition and its effect on the quality of diffusion bonds is still missing. Knowing these factors helps us to design structural parts with higher strength.

Up to the present, ample works have been devoted to the phenomenical description of the diffusion bonding process, especially on the kinetics of void evolution. Yakushina et al. [22] found that the bonding cavities gradually disappeared as the bonding time increased from 2 to 4 h at 725 °C. Many studies reported that, compared to coarse-grained materials, void shrinkage is evident in fine-grained alloys under the identical experimental condition of pressure, temperature, and time [23]. Therefore, fine-grained alloys give better joint strength and the bonding pressure is relatively low. However, the underlying binding mechanism is still unclear for fine-grained materials. The atomic diffusion process and grain boundary migration mechanism during diffusion bonding is different for alloys with different grains sizes.

The purpose of this paper is to explore the variation of grain size on the mechanical behaviors and bonding mechanism of SP700 alloy. The SP700 alloy was heat-treated at different time points, and then the material was used for diffusion bonding under the same experimental condition. Tensile tests were performed to evaluate the quality of the bonds. The bonding mechanism of the alloy for different microstructures is discussed in the end.

2. Materials and Methods

The researched SP700 sheets used in this paper were rolling titanium sheets, which were supplied by the Avic Xi'an Aircraft Industry Group Company Ltd., Xi'an, China. The chemical compositions of the SP700 alloy were obtained by inductively coupled plasma–optical emission spectrometry (ICP-OES), as shown in Table 1. The nominal composition of SP700 is Ti-4.5Al-3V-2Mo-2Fe, which is based on Ti-6Al-4V with the addition of β-stabilizing elements (Mo and Fe). Mo elements in titanium can refine the microstructure and inhibit grain growth at high temperatures.

Table 1. Chemical compositions of the SP700 alloy.

Chemistry (wt.%)	Ti	Al	V	Fe	Mo
SP700	Bal.	4.3	3.06	1.79	2.12

To produce different grain size distribution, heat treatments were conducted at 825 °C for 50 min under an argon atmosphere. After heat treatments, the SP700 sheets and the initial materials were polished for diffusion bonding to evaluate the effect of grain size on the diffusion properties. The diffusion bonding process was carried out in the ZRY55 vacuum hot-press furnace (Shaanxi Material Analysis and Research Center, Xi'an, China), the vacuum degree during the experiment was 1×10^{-2} Pa. The diffusion bonded samples for the tensile tests were cut from rectangular sheets, and the length and width were 1400 mm and 800 mm, respectively. Diffusion bonding was performed for 2 h at 825 °C while applying a pressure of about 2 MPa. Tensile specimens with gauge dimensions of 60 mm (L) × 15 mm (W) × 2 mm (T) were sectioned in the rolling direction by spark machining, as is shown in Figure 1. Tensile tests were performed on the Instron-5500R testing machine at a temperature ranging from 350 to 400 °C at a strain rate of 1×10^{-3} s^{-1}. Each test has designed to be repeated three times. The microstructures of specimens after diffusion bonding were characterized using the optical microscope (OM) (Shaanxi Material Analysis and Research Center, Xi'an, China). The fracture surface and bonding interface of the bonds were observed by an FEI NanoSEM 430 scanning electron microscope (Shaanxi Material Analysis and Research Center, Xi'an, China).

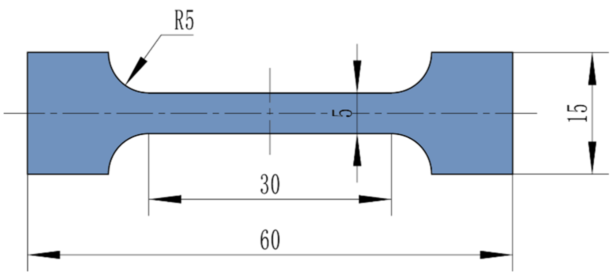

Figure 1. The dimensions of the tensile specimen (mm).

3. Results

3.1. The Microstructure Observation Results

Figure 2a gives the inverse pole figure (IPF) of the as-received material with respect to the transverse direction (TD). It can be observed that the initial material, which contains a 96.2% α phase, keeps lath-like and some grains are oriented with their c-axis parallel to TD. The pole figure of Figure 2b confirms the existence of rolling texture and the <0001> directions of α phase are nearly parallel to the TD, which are often found in α titanium alloys. The grain boundary misorientation map in Figure 2c illustrates that most of grain boundary is low angle grain boundary (<15°). Some high angle grain boundary in this figure may indicate the initiation of the tensile and/or compressive twinning during hot rolling. Figure 3a shows the IPF of the heat-treated specimen, and grain growth is evident in Figure 3a. The basal texture can still be observed in Figure 3b. The grain boundary misorientation map in Figure 3c is similar to the trend observed in Figure 2c. This demonstrates that the initial material and heat-treated specimen has similar grain misorientation distribution, but different grain size.

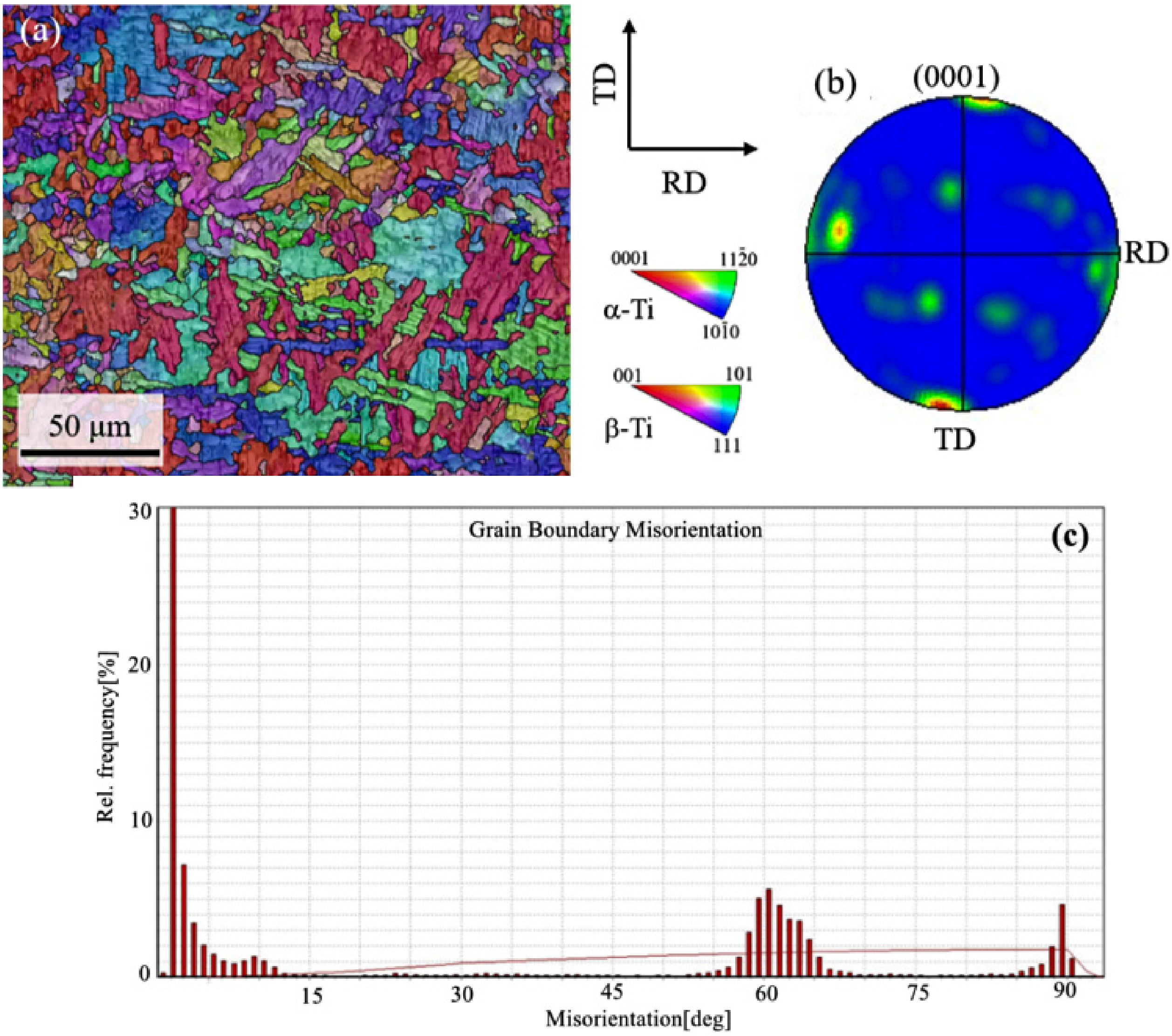

Figure 2. (**a**) Inverse pole figure along the transverse direction; (**b**) Pole figure and (**c**) grain boundary misorientation distribution of the initial material.

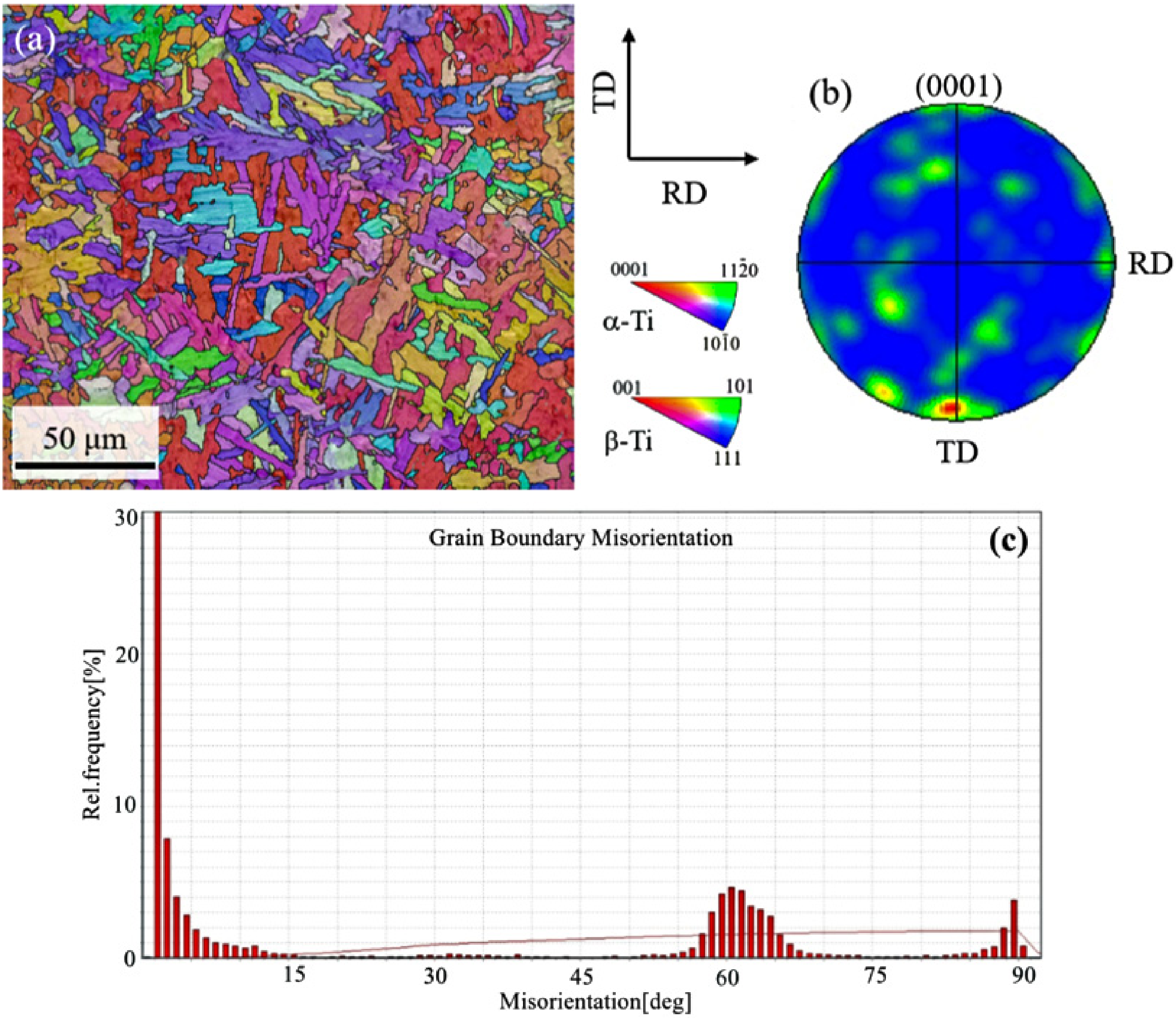

Figure 3. (**a**) Inverse pole figure along the transverse direction; (**b**) Pole figure and (**c**) grain boundary misorientation distribution of the heat-treated specimen.

3.2. Mechanical Properties of the SP700 at Elevated Temperature

Figure 4 gives the engineering stress–true strain curves for the SP700 alloy with and/or without heat treatment. All of the tensile specimens fracture at the bonding interface. From Figure 4, it can be concluded that the initial material has higher elongation compared with the heat-treated specimen and there is no significant difference in tensile strength between these two materials. For example, as seen from Figure 4a,b, the elongation of the initial SP700 sheet was 23% at the temperature of 350 °C while the ductility of the heat-treated specimen decreased to 16%. Similar trends are also observed at 400 °C in Figure 4c,d. It should be noted that these two materials have the same processing history, but different grain sizes. Therefore, the difference in ductility between these two specimens indicates that the variation of grain size has a significant effect on the diffusion bonding properties. The size of the grains in a polycrystalline metal influences the mechanical properties. It is generally accepted that a fine-grained material is harder and stronger than one that is coarsed grained, because the former has a great total grain boundary area to impede dislocation motion and grain size reduction improves not only the strength, but also the toughness of many alloy. The reason why these two alloys have similar strength is that these two specimens contain abundant low angle grain boundaries, as indicated in Figures 2c and 3c, and small-angle grain boundaries are not effective in interfering with the slip process because of the slight crystallographic misalignment across the boundary.

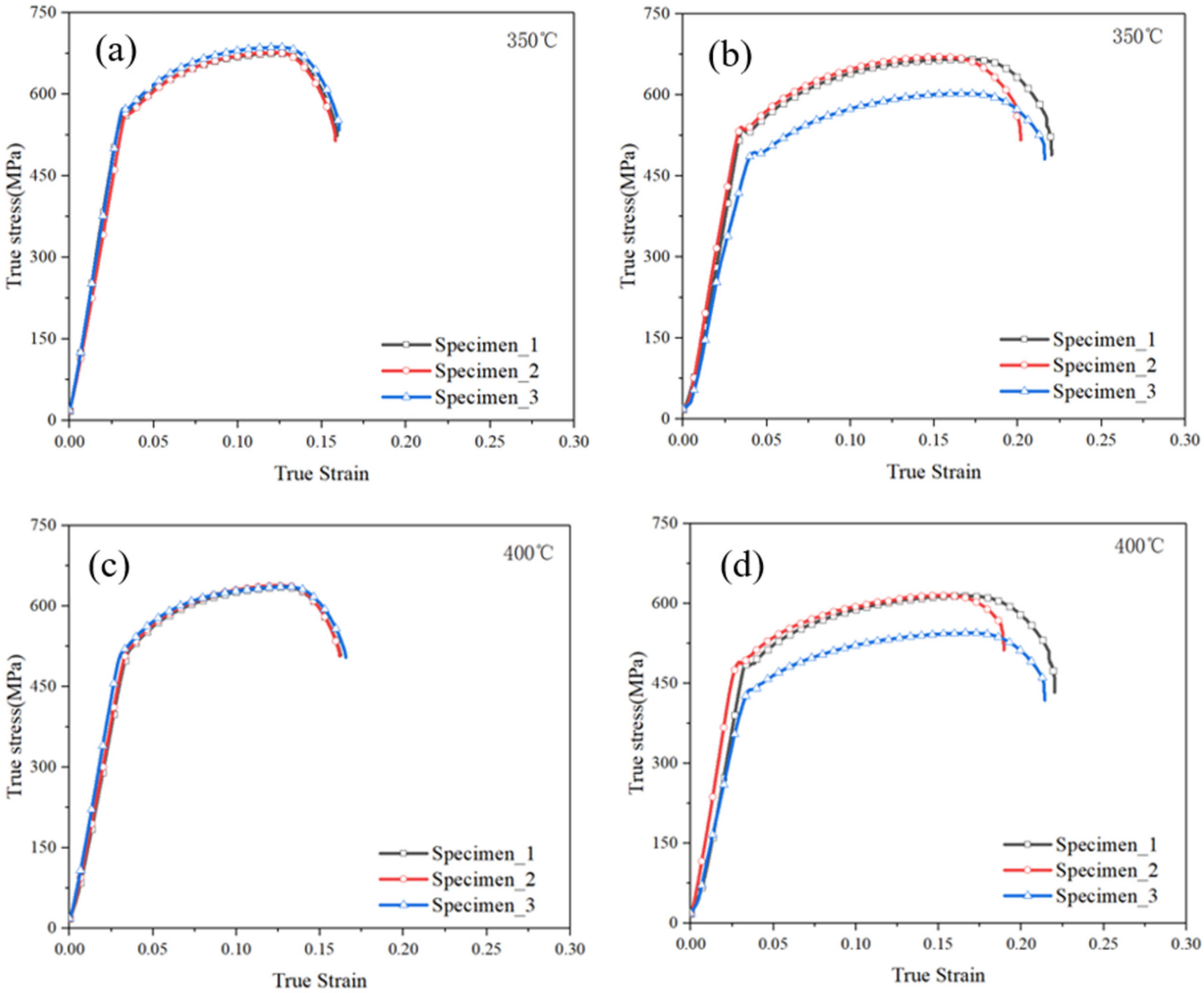

Figure 4. The stress–strain curve of the heat-treated SP700 alloy at (**a**) 350 °C and (**c**) 400 °C when the diffusion bonding process is done. The engineering stress–strain curves of the initial alloy at (**b**) 350 °C and (**d**) 400 °C after diffusion bonding.

3.3. Microstructure and Grain Size at the Bonding Interface

Many factors are affecting the bonding strength of the SP700 alloy. The bonding temperature, time, and bonding pressure were the same for the initial material and heat-treated specimen; the only difference is that these two specimens have different grain sizes. Figure 5 gives the SEM images of the bonding interfaces for the initial material and heat-treated alloys, respectively. For the initial material, there is a visible diffusion interface in Figure 5a,b. However, a discontinuity area was found at the bond interface for the heated-treated specimen, as indicated in Figure 5c,d. The bonding condition in Figure 5b,d explains the difference in elongation in Figure 4 for these two alloys. The different bonding conditions are associated with the grain-boundary migration, which is discussed in detail in Section 4.2.

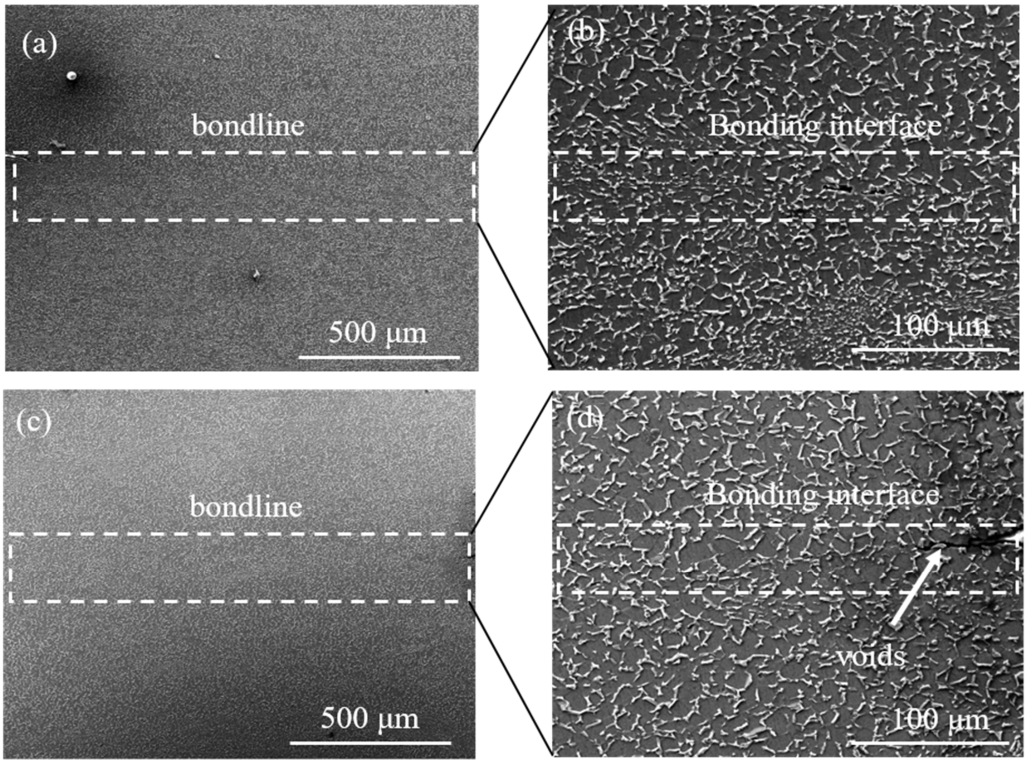

Figure 5. (**a**,**b**) SEM images of the bond interface for initial SP700 alloy; (**c**,**d**) Microstructure of the heat-treated alloy after diffusion bonding.

Figure 6 depicts the grain structure of the initial materials and heat-treated specimen after diffusion bonding. Compared with grains in Figure 6a, it is evident that significant grain growth occurs in the heat-treated specimen, as indicated in Figure 6c. The grain size was determined using the linear intercept method. The grain size of the initial material in Figure 6b is estimated to be 3 μm, while this value is determined to be 10 μm in the heat-treated specimen. Grain growth occurs by the migration of grain boundaries and boundary motion is just the short-range diffusion of atoms from one side of the boundary to the other. Energy is associated with grain boundaries. As grains increase in size, the total boundary area decreases, yielding an attendant reduction in the total energy. Thus, compared with one that is coarse-grained, a fine-grained material can readily move during diffusion bonding.

3.4. Fracture of the Tensile Specimens

Much more detailed information regarding the mechanism of fracture is available from microscopic examination using SEM. Figure 7 gives the fractographic images of the initial material and heat-treated specimen after the tensile specimen at 400 °C. As illustrated in Figure 7a–c, when the fracture surface of the initial material is examined at high magnification, it is found to consist of many spherical dimples and the dimension of the dimples ranges from 2 μm to 5 μm. This structure is characteristic of fracture resulting from the uniaxial tensile failure. Each dimple is one-half of a microvoid that formed and then separated during the fracture process. Dimples also form on the heat-treated specimen, as indicated in Figure 7d–f. However, dimples on the heated-treated specimen have large dimensions, 20 μm to 100 μm, compared with that in Figure 7a–c. Similar trends were also observed at 350 °C, where tiny dimples form on the fracture surface of the initial materials. The fracturegraph in Figure 7 provides valuable information in the analyses of fracture, such as fracture mode, the stress state, and the site of crack initiation.

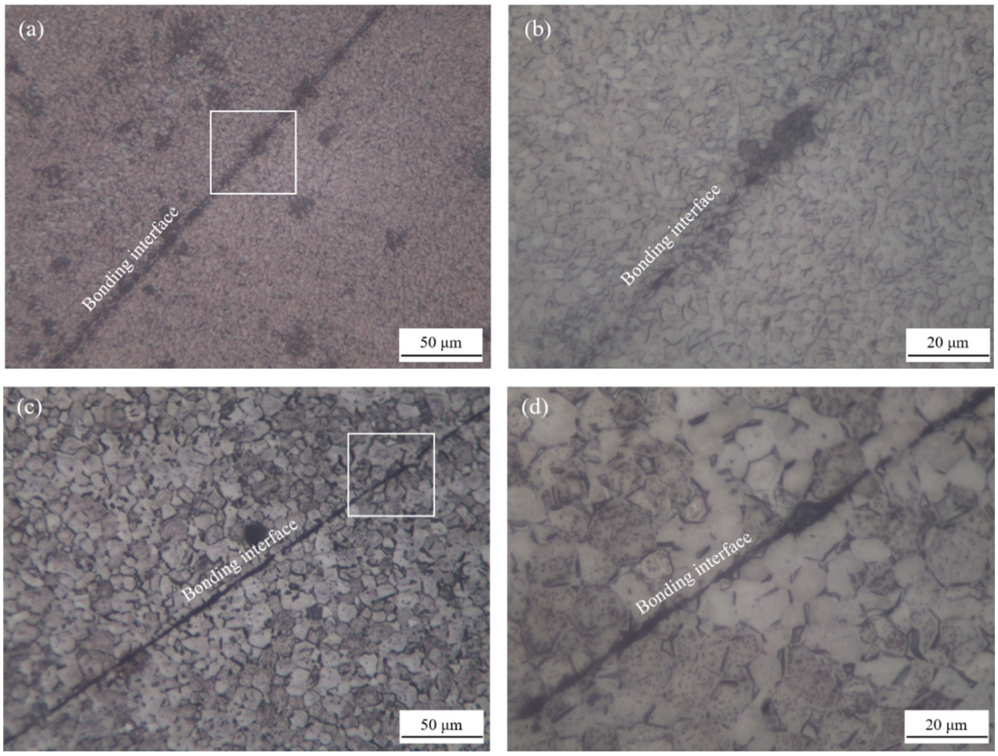

Figure 6. (**a**) Grain structure at the bonding interface for the initial materials; (**b**) high magnification of the square insets in Figure 6a. (**c**) Grain morphology of the heat-treated specimen at the bonding interface; (**d**) high magnification of to the square insets in Figure 6c.

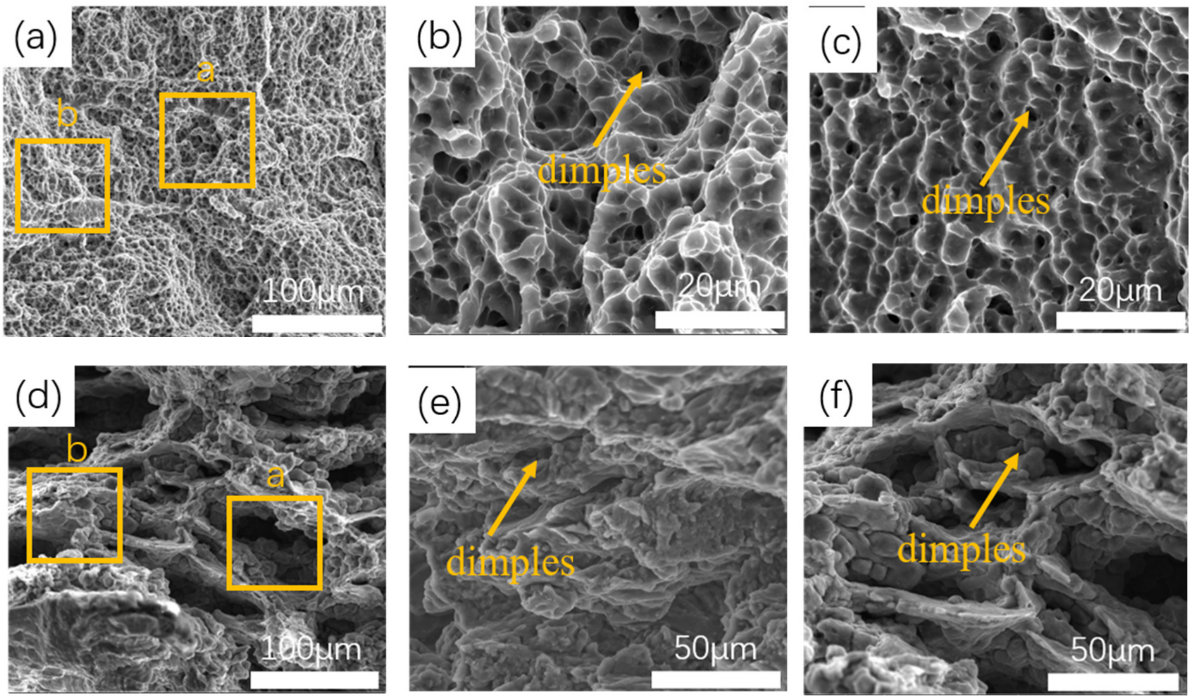

Figure 7. Scanning electron fractographic showing spherical dimples characteristic of ductile fracture resulting from uniaxial tensile loading. (**a**) The fracture morphology of the initial material at 400 °C. (**b**,**c**) High magnification image of the square insets in Figure 5a. (**d**) The fracture morphology of the heat-treated specimen at 400 °C. (**e**,**f**) High magnification image of the square insets in Figure 5d.

4. Discussions

4.1. The Mechanisms of the Micro-Cracks Nucleation

As is shown in Figure 8, for the microstructural evolution, the quality of the DB process is mainly due to the grain sizes of initial materials. The smaller the grain size, the fewer the micro-cracks and the better the weldability of the material. For the coarse-grained titanium alloys, there are many microscopic cracks between the grains in the diffusion joint, which is the main cause of the degradation of the mechanical properties after diffusion. The micro-cracks of the bonding joints are mainly caused by the following microstructure evolutions:

(i) If the gap distances between two grains of sheet A are less than the grain sizes of sheet B, it is difficult for the grains in B to diffuse into plate A. This would cause inhomogeneity at the diffusion interfaces, and cracks prefer to form at locations with small gap distances;
(ii) When the grains on both sides reach the boundaries, and the middle grains have a distance of h_1 or then h_2 from the boundary, an arc-shaped PRQ will be formed, which is the reason for the inhomogeneous diffusion interface;
(iii) Grain boundary sliding (GBS) also can cause the inconsistency in atomic diffusion between different grains, which is also affected by the grain sizes.

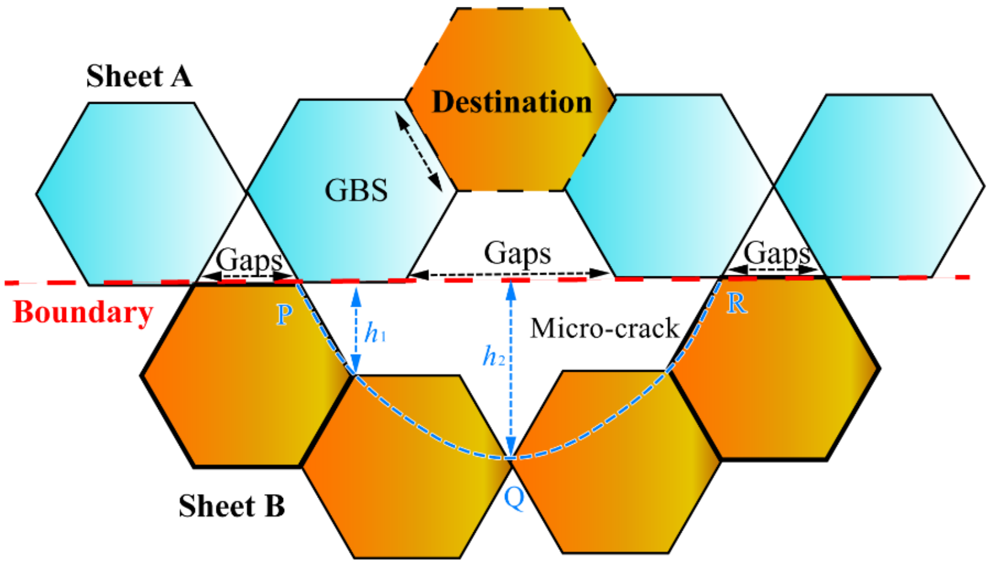

Figure 8. The mechanisms of micro-cracks during the DB process of titanium alloy.

In summary, the nature of crack nucleation is caused by the inhomogeneity of atomic diffusion, and the formation of micro-cracks in diffusion connections is directly related to the grain sizes and grain gap distances.

4.2. The Difference in the Mechanical Properties between Initial and Heat-Treated Material

Based on the results above, it is possible to map the diffusion bonding process for the different SP700 alloys in this research, as represented schematically in Figure 9. The solid-state bond created between two SP700 alloys is so well-formed that it is usually difficult to detect the original interface in Figure 5. One of the reasons that a good solid-state bond can be readily established between two titanium sheets is attributed to the fact that Ti has extensive solid solubility (~34 at.% in α-Ti) for oxygen at high temperatures (greater than 825 °C) where superplasticity takes place. At diffusion bonding temperature, the Ti surface oxide is dissolved, resulting in extensive interdiffusion across the bond interface, and giving rise to a good metallurgical bond. However, this favorable situation does not normally exist in other metal alloys.

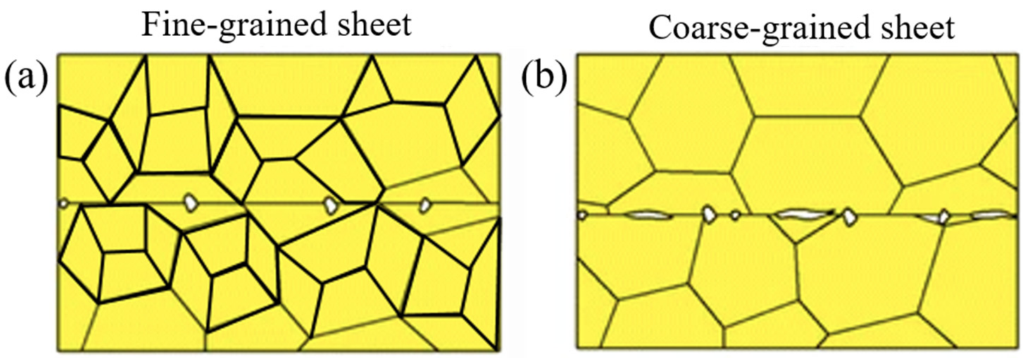

Figure 9. Schematic illustration of the diffusion bonding process for the (**a**) fine-grained and (**b**) coarse-grained alloys.

Under the same bonding conditions, an important property of fine-grained SP700 alloy is that they can often be readily bonded in the solid-state. Thus, the ductility of the initial material is higher than that of the coarse-grained specimen in Figure 4. This type of bonding is possible because of the presence of many grain boundaries in fine-grained materials that act as short-circuit paths for diffusion, as illustrated in Figure 9a. Moreover, at bonding temperature, diffusion process, and particularly grain-boundary diffusion, usually are rapid, permitting extensively boundary migration and void shrinkage occurring at the interface. Thus, grain boundary migration is faster in fine-grained than in coarse-grained materials in Figure 9. The same materials, if coarse-grained, may not readily bond under identical conditions of pressure, temperature, and time.

4.3. The Fracture Mechanism for the Initial and Heat-Treated Material

Much more detailed information regarding the mechanism of fracture is available from fractographic studies using SEM, as indicated in Figures 7 and 8. These characteristics are necessary to reveal the topographical feature of fracture surfaces and other information, such as the fracture mode, the stress state, and the site of crack initiation. The fracture surface of a heat-treated specimen is quite different from those of the initial specimen after diffusion bonding. A direct comparison between two fracture surfaces tested at the same temperature in Figures 7 and 8 indicates that dimples on the heated-treated specimen have large dimensions compared with that in the initial material. The fracture process normally occurs in several stages. First, after necking begins, small cavities, or microvoids, form in the interior of the cross-section, as indicated in Figure 10b. Next, as deformation continues in Figure 10c, these microvoids enlarge, come together, and coalesce to form an elliptical crack, which has its long axis perpendicular to the stress direction. Finally, fracture ensues by the rapid propagation of a crack around the neck by shear deformation (Figure 10d,e). Generally, the greater the load, the greater the proximity and total gap volume of these dimples. The presence of large dimples on the fracture surface for the heated-treated specimen demonstrates that heterogeneous deformation develops during tension, suggesting substantial debonding during the diffusion bonding. The fracture surface appearance on the initial material can be interpreted as a result of extensive bonding between two SP700 sheets.

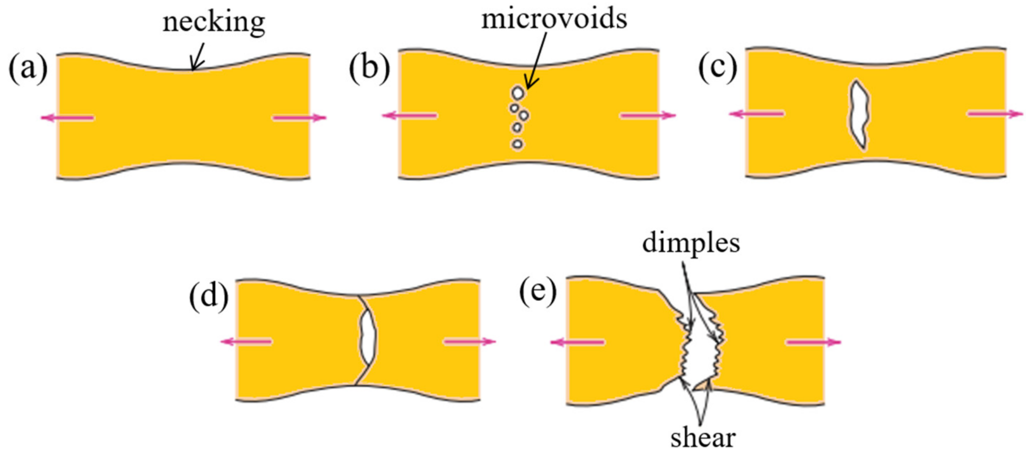

Figure 10. Stages in the ductile fracture. (**a**) Initial necking. (**b**) Small cavity formation. (**c**) Coalescences of cavities to form a crack. (**d**) Crack propagation. (**e**) Final shear fracture.

5. Conclusions

This research aimed to investigate the effect of grain size on the diffusion bonding performance for the SP700 alloy. The mechanical properties of the initial materials and heat-treated specimen after diffusion bonding were evaluated by tensile test. The main conclusions are as follows:

1. The initial material has higher elongation compared with the heat-treated specimen and there is no significant difference in tensile strength between these two materials.
2. The same materials, if coarse-grained, may not readily bond under identical conditions of pressure, temperature, and time.
3. Grain boundary migration is faster in fine-grained than in coarse-grained materials. The presence of many grain boundaries in fine-grained materials acts as short-circuit paths for diffusion.
4. The dimples on the heated-treated specimen have large dimensions compared with that in the initial material, indicating that heterogeneous deformation develops in the coarse-grained specimen during tension.

Author Contributions: Q.Z.: conceptualization, experimental investigations, programing, theoretical calculations, analysis, and writing—original draft. J.W.: analysis, writing—review & editing, and supervision. S.J.: experimental investigations, discussion & review. G.H.: writing—review & editing. All authors have read and agreed to the published version of the manuscript.

Funding: No funding supports this research.

Institutional Review Board Statement: Not applicable.

Informed Consent Statement: Not applicable.

Data Availability Statement: Not applicable.

Acknowledgments: The authors thank Northwestern Polytechnical University for providing the research infrastructure and the Harbin Institute of Technology for their help with the experiments.

Conflicts of Interest: We declare that we have no financial and personal relationships with other people or organizations that can inappropriately influence our work, there is no professional or other personal interest of any nature or kind in any product, service, and/or company that could be construed as influencing the position presented in, or the review of, the manuscript entitled, “The Effect of Grain Size on the Diffusion Bonding Properties of SP700 Alloy”.

References

1. Guo, Y.; Liu, R.; Arab, A.; Zhou, Q.; Guo, B.; Ren, Y.; Chen, W.; Ran, C.; Chen, P. Dynamic behavior and adiabatic shearing formation of the commercially pure titanium with explosion-induced gradient microstructure. *Mater. Sci. Eng. A* **2022**, *833*, 142340. [CrossRef]
2. Yang, J.; Wu, J. Grain rotation accommodated GBS mechanism for the Ti-6Al-4V alloy during superplastic deformation. *Crystals* **2021**, *11*, 991. [CrossRef]
3. Alabort, E.; Barba, D.; Shagiev, M.R.; Murzinova, M.A.; Galeyev, R.M.; Valiakhmetov, O.R.; Aletdinov, A.F.; Reed, R.C. Alloys-by-design: Application to titanium alloys for optimal superplasticity. *Acta Mater.* **2019**, *178*, 275–287. [CrossRef]
4. Zhang, R.; Shao, Z.; Lin, J. A review on modelling techniques for formability prediction of sheet metal forming. *Int. J. Light. Mater. Manuf.* **2018**, *1*, 115–125. [CrossRef]
5. Wu, Y.; Wu, D.; Ma, J.; Xiao, W.; Zheng, K.; Chen, M. A physically based constitutive model of Ti-6Al-4 V and application in the SPF/DB process for a pyramid lattice sandwich panel. *Arch. Civ. Mech. Eng.* **2021**, *21*, 106. [CrossRef]
6. Mosleh, A.O.; Kotov, A.D.; Vidal, V.; Mochugovskiy, A.G.; Velay, V.; Mikhaylovskaya, A.V. Initial microstructure influence on Ti–Al–Mo–V alloy's superplastic deformation behavior and deformation mechanisms. *Mater. Sci. Eng. A* **2021**, *802*, 140626. [CrossRef]
7. Yasmeen, T.; Zhao, B.; Zheng, J.H.; Tian, F.; Lin, J.; Jiang, J. The study of flow behavior and governing mechanisms of a titanium alloy during superplastic forming. *Mater. Sci. Eng. A* **2020**, *788*, 139482. [CrossRef]
8. Zhang, T.; Sha, H.; Li, L.; Gong, H. Study of Macroscopic Defects of Four-Layer Structure of Ti–6Al–4V During Superplastic Forming/Diffusion Bonding. *Int. J. Precis. Eng. Manuf.* **2021**, *22*, 27–39. [CrossRef]
9. Gao, W.; Xing, S.; Lei, J. Effect of bonding temperature and holding time on properties of hollow structure diffusion bonded joints of TC4 alloy. *SN Appl. Sci.* **2020**, *2*, 1960. [CrossRef]
10. Zeng, S.; You, G.; Yao, F.; Luo, J.; Tong, X. Effect of bonding temperature on the microstructure and mechanical properties of the diffusion-bonded joints of Zr705 alloy. *Mater. Sci. Eng. A* **2021**, *804*, 140782. [CrossRef]
11. García-Barrachina, L.; Gámez, A.J. Dimensional analysis of superplastic processes with the buckingham Π theorem. *Metals* **2020**, *10*, 1575. [CrossRef]
12. Sorgente, D.; Palumbo, G.; Piccininni, A.; Guglielmi, P.; Tricarico, L. Modelling the superplastic behaviour of the Ti6Al4V-ELI by means of a numerical/experimental approach. *Int. J. Adv. Manuf. Technol.* **2017**, *90*, 1–10. [CrossRef]
13. García-Barrachina, L.; Gámez, A.J.; Marcos, M. Dimensional analysis of superplastic bulge forming. *Procedia Manuf.* **2017**, *13*, 364–371. [CrossRef]
14. Mosleh, A.O.; Kotov, A.D.; Mestre-Rinn, P.; Mikhaylovskaya, A.V. Superplastic forming of Ti-4Al-3Mo-1V alloy: Flow behavior modelling and finite element simulation. *Procedia Manuf.* **2019**, *37*, 239–246. [CrossRef]
15. Yang, J.; Wu, J.; Zhang, Q.; Han, R.; Wang, K. Investigation of flow behavior and microstructure of Ti–6Al–4V with annealing treatment during superplastic forming. *Mater. Sci. Eng. A* **2020**, *797*, 140046. [CrossRef]
16. Chandrappa, K.; Kant, R.; Ali, R.; Vineth, K. Optimization of process parameter of diffusion bonding of Ti-Al and Ti-Cu. *Mater. Today Proc.* **2020**, *27*, 1689–1695. [CrossRef]
17. Du, Z.; Zhang, K.; Lu, Z.; Jiang, S. Microstructure and mechanical properties of vacuum diffusion bonding joints for γ-TiAl based alloy. *Vacuum* **2018**, *150*, 96–104. [CrossRef]
18. Zhu, L.; Li, J.; Tang, B.; Liu, Y.; Zhang, M.; Li, L.; Kou, H. Microstructure evolution and mechanical properties of diffusion bonding high Nb containing TiAl alloy to Ti 2 AlNb alloy. *Vacuum* **2019**, *164*, 140–148. [CrossRef]
19. Zhang, H.; Li, J.; Ma, P.; Xiong, J.; Zhang, F. Study on microstructure and impact toughness of TC4 titanium alloy diffusion bonding joint. *Vacuum* **2018**, *152*, 272–277. [CrossRef]
20. Lin, Z.-R.; Zhang, Z.-Y.; Huang, W.-D. An investigation of diffusion bonding under superplastic condition for Ti-6A-4V Titanium alloys. *Chin. J. Aeronaut.* **1993**, *6*, 228–237.
21. Han, D.; Zhao, Y.; Zeng, W. Effect of Zr addition on the mechanical properties and superplasticity of a forged SP700 titanium alloy. *Materials* **2021**, *14*, 906. [CrossRef] [PubMed]
22. Yakushina, E.; Reshetov, A.; Semenova, I.; Polyakova, V.; Rosochowski, A.; Valiev, R. The influence of the microstructure morphology of two phase Ti-6Al-4V alloy on the mechanical properties of diffusion bonded joints. *Mater. Sci. Eng. A* **2018**, *726*, 251–258. [CrossRef]
23. Wang, K.; Wang, L.; Zheng, K.; He, Z.; Politis, D.J.; Liu, G.; Yuan, S. High-efficiency forming processes for complex thin-walled titanium alloys components: State-of-the-art and perspectives. *Int. J. Extrem. Manuf.* **2020**, *2*, 032001. [CrossRef]